it is possible to predict from this study that single-kernel differences would be heritable and that breeding programs, such as mass selection and single recurrent selection which make use of high heritability, would probably be effective for modification of corn oil quality. Consequently, a high-resolution NMR selection technique for unsaturation may prove as advantageous as the wide-line NMR single-kernel technique in speeding the development of new corn strains.

In 1962 Johnson and Shoolery (*8*) described a high-resolution NMR method for determining the average molecular weight and iodine value of natural fats dissolved in carbon tetrachloride. With this method the NMR integral signal from C(1) and C(3) glyceride protons provides an internal standard from which the olefinic and total number of hydrogen atoms are measured. From these, an average molecular weight and iodine value are calculated. Agreement between NMR and Wijs iodine values is remarkably good.

To demonstrate viability under the conditions of our method, we dried whole kernels of 25 commercial corn hybrids to 4 percent moisture and subjected them to 95°C for periods up to 90 minutes. Others were soaked in Freon-113 for periods up to 6 days. Subsequent germination tests showed a high degree of tolerance to low moisture heating (94 percent survival) and to the solvent treatment (98 percent survival).

For NMR experiments proposed earlier (*9*), individual corn kernels or excised germ were mounted on a Teflon-glass pedestal, transferred to 12-mm tubes and covered with Freon-113 to minimize the large discontinuities in magnetic susceptibilities within the sample cell. Samples were examined with a Varian model HA-100-15 high-resolution spectrometer equipped with a wide gap magnet. Typical spectra from kernels of commercial-dried (15 percent corn moisture), laboratory-dried (4 percent corn moisture), and laboratory-dried corn soaked in Freon-113 for 6 days are shown in Fig. 1 with NMR chemical shift assignments. The spectrum from the commercial-dried kernel (Fig. 1A) was not usable because of the broad absorption signal. The laboratory-dried kernel (Fig. 1B) exhibited a poor NMR spectrum; resolution and signal-to-noise ratio were less than satisfactory. Surprisingly, heating the dry sample up to 95°C to alter the mobility of the fat did not improve resolution. By contrast, solvent treatment of dried seeds altered the mobility of the oil sufficiently to provide very good signal-to-noise ratios and adequate resolution to separate the olefinic and glyceride methylene protons (Fig. 1C). Proper integration of spectra from single seeds permits determination of iodine value and average molecular weight by means of the Johnson-Shoolery (*8*) calculation. These data indicate that sample drying and solvent treatment are necessary to obtain usable spectra. Variations in NMR spectra resolution have been observed between seeds which are attributed to differences in magnetic susceptibilities between the oil and the corn germ matrix as well as between the seed and surrounding solvent. Minimizing these should improve spectra resolution.

The spectra shown in Fig. 1 were obtained with 250-second sweep time. Through use of NMR radio-frequency pulse techniques and Fourier transformation of the data (*10*), it is possible to greatly reduce instrument time. Studies with the Varian FT-100 Fourier transform accessory (Fig. 2) show a 10-second examination of an excised corn germ which was fitted into a 5-mm tube and surrounded by Freon-113. These results suggest that unsaturation in the whole kernel can be measured in times as short as 10 seconds.

T. F. CONWAY
*George M. Moffett Research Laboratories, Corn Products Company, Argo, Illinois*

L. F. JOHNSON
*Instrument Division, Varian Associates, Palo Alto, California*

**References and Notes**

1. T. F. Conway and R. J. Smith, in *Developments in Applied Spectroscopy*, J. R. Ferraro and J. S. Ziomek, Eds. (Plenum Press, New York, 1963), p. 115; D. E. Alexander, L. Silvela S., F. I. Collins, R. C. Rogers, *J. Amer. Oil Chem. Soc.* **44**, 555 (1967).
2. I. Zupančič *et al.*, *Acta Chem. Scand.* **21**, 1664 (1967).
3. L. F. Bauman, T. F. Conway, S. A. Watson, *Science* **139**, 498 (1963); *Crop Science* **5**, 137 (1965).
4. J. Dumanović and V. Trifunović, *Contemp. Agr.* (Novi Sad) **7-8**, 521 (1964).
5. L. Silvela S., "Improvement in recurrent selection methods for oil in maize through nuclear magnetic resonance analysis," thesis, University of Illinois, Urbana (1965).
6. B. Brimhall and G. F. Sprague, *Cereal Chem.* **28**, 225 (1951).
7. C. G. Poneleit, "Diallel analysis of fatty acids in corn (*Zea mays* L.) oil," thesis, Purdue University, Lafayette, Ind. (1968).
8. L. F. Johnson and J. N. Shoolery, *Anal. Chem.* **34**, 1136 (1962).
9. A. L. Elder, D. M. Rathmann, T. F. Conway, *Qual. Plant. Mat. Veg.* **15**, 67 (1964).
10. R. R. Ernst, in *Advances in Magnetic Resonance*, J. S. Waugh, Ed. (Academic Press, New York, 1966), vol. 2, p. 108.

9 January 1969

## Simultaneously Recorded Trains of Action Potentials: Analysis and Functional Interpretation

Abstract. *A new kind of statistical display, the joint peri-stimulus-time scatter diagram, facilitates the analysis and interpretation of two or more simultaneously recorded trains of action potentials. The display is a generalization of the cross correlation and the peri-stimulus-time histogram, and it reflects specific underlying neuronal interactions. The technique yields quantitative measures of interaction in terms of effectiveness of synaptic connections.*

Much of the known picture of the nervous system has been obtained from single neurons individually studied for an extended period of time. On the other hand, anatomical, physiological, and behavioral evidence overwhelmingly suggest that integrative functions in the nervous system are performed by simultaneous activity in groups of neurons. It has become possible to record several trains of action potentials (spike trains) simultaneously and to analyze their temporal relationships. The results of these analyses may, in turn, be interpreted in terms of connections which underlie the integrative process in the group of neurons under observation (*1*, *2*). We describe here a method of performing such analyses for experiments in which a repeated stimulus is presented to a system of neurons and in which two or more spike trains are simultaneously monitored. This method is more powerful and sensitive than that suggested by Perkel *et al.* (*2*, p. 429) and permits a relatively direct functional interpretation.

Our basic data consist of the times of occurrence of three sets of events: a train of periodic (identical) stimuli, and two trains of action potentials (A and B). Let the time of occurrence of the $i$th stimulus be $S_i$; that of the $j$th spike of train A be $A_j$; and that of the $k$th spike of train B be $B_k$. We con-

struct a scatter diagram of the joint occurrences of spikes in trains A and B relative to the times of stimulation. Thus, the ordinate of each point plotted corresponds to the time between a stimulus event and a spike in A (for example, $A_j - S_i$), and the abscissa corresponds to the time between the same stimulus event and a spike in B (for example, $B_k - S_i$). For each stimulus event, a point is plotted for each combination of S-A and S-B intervals, both of which fall within a specified range. Thus, in general, a spike in train A will give rise to as many points in the scatter diagram as there are spikes in train B within the specified time range about the stimulus (and vice versa). This computation and plot have been done with a Linc computer as well as with considerably larger machines.

We call this plot the joint peri-stimulus-time (PST) scatter diagram (*3*) (Figs. 1 and 2). In fact, the scatter diagram represents an estimate of an underlying joint PST density; the two PST histograms estimate a related set of marginal densities (*4*).

The scatter diagram represents a generalization of the PST histograms of each of the two spike trains, and of the cross-correlation histogram. If we impose a square grid of convenient spacing over the scatter diagram, then the set of tallies by columns is related to the PST histogram of train B, and the corresponding set of tallies by rows is related to the PST histogram of train A. Furthermore, tallies along the direction parallel to the principal diagonal are proportional to the cross-correlation histogram, with a suitable normalization of the time axis. The scatter diagram contains information beyond that provided by the two PST and the cross-correlation histograms and cannot be reconstructed from these histograms alone, no matter how fine the resolution.

Each of the several possible types of functional connection to and between the observed neurons produces a characteristic signature in the scatter diagram. For example, two independently firing neurons which are totally unaffected by the stimulus will produce a uniform scatter of points. If, in addition, the stimulus produces an increase in firing probability at fixed latency in neuron A only (such as would be produced by an excitatory synaptic pathway), then a horizontal band of higher point density will be seen in the scatter diagram. The location of the band is a measure of the latency of the excitation; the width and structure of the band depend on the details of the excitatory mechanism. If the stimulus produces a fixed latency decrease in firing probability of neuron A (for example, due to synaptic inhibition) there will be a horizontal band of lower point density than the general background density in the scatter diagram. If the stimulus affects neuron B and not neuron A, then only a corresponding set of vertical bands will be produced.

A direct synaptic pathway from neuron A to neuron B will produce a 45° band of different density lying below the principal diagonal at a distance proportional to the latency of the interaction. A synaptic pathway from neuron B to neuron A will produce a similar band lying above the principal diagonal.

If the synaptic pathways between A and B can be affected by the stimulus (as by stimulus influence on an interneuron), then the diagonal band will show changes in density along its length. For example, if the stimulus inhibits an excitatory interneuron between A and B, the diagonal band will be reduced in density over a segment corresponding to the latency and duration of the inhibition (Fig. 1).

A final principal class of interaction is represented by a shared source of input to A and B which is independent of the stimulus. This gives rise to a diagonal band which is difficult to distinguish qualitatively from the diagonal band produced by a direct excitatory pathway from A to B or from B to A. However, for a given strength of synapse, shared excitatory input produces a much less dense and a wider band than a direct synaptic connection between the two neurons. The density difference and other structural details of the band usually enable a choice to be made between the alternatives (*2*, p. 431). If such a source of shared input is itself modified in a time-locked way by the stimulus, these modifications will be reflected in density changes along the diagonal band.

If combinations of these elementary influences occur, each of the corresponding bands will ordinarily appear in the scatter diagram (Figs. 1 and 2). The scatter diagram can yield quantitative estimates of synaptic effectiveness in the inferred connections between neurons if the points within particular bands and band intersections are counted.

We may estimate the contributions

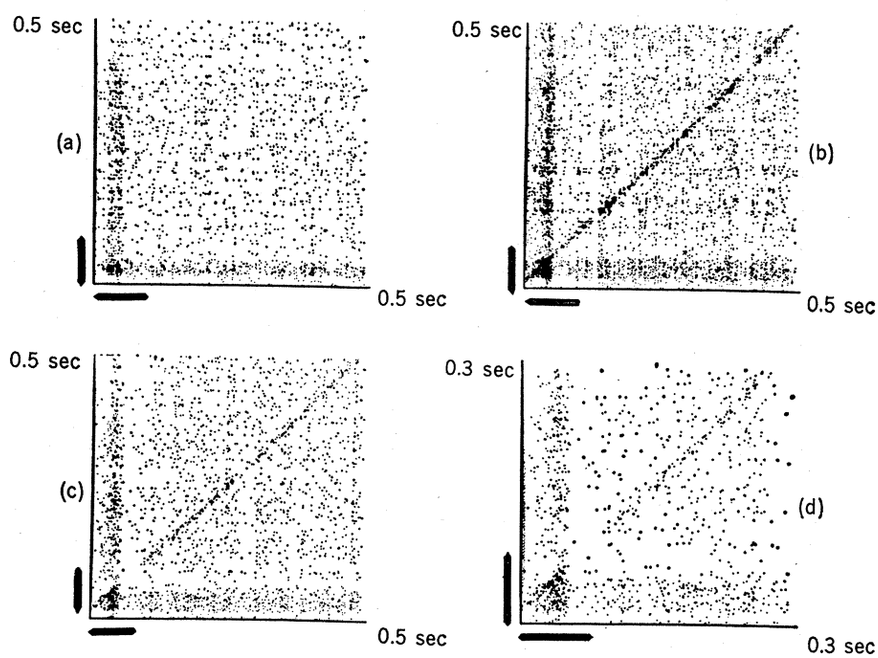


Fig. 1. Joint PST scatter diagrams in computer-simulated neural networks. (a) Neurons 1 and 2 with common excitatory followed by inhibitory input from a periodic stimulus. Duration of the stimulus is indicated by dark bars. Note vertical and horizontal bands of higher density. (b) Same situation as (a) but with added excitatory interaction from neuron 1 to neuron 2. Note diagonal band of higher density. (c) Same situation as (b) except that the excitatory interaction from neuron 1 to neuron 2 is itself inhibited by the stimulus. In contrast to (b) the diagonal band is interrupted during the latter portions of stimulus. (d) Enlargement of lower left region of (c). Details of each band structure allow inference about various synaptic input sequences.

of only the direct stimulus effects to the scatter diagram by constructing the cross product of the marginal probability densities (obtained from the two PST histograms). The resulting bivariate density, which contains no diagonal bands, serves as a control. It represents the hypothetical case in which the two neurons fire independently except for shared input caused by the stimulus. Comparison of this control with the observed joint density facilitates the detection of direct interactions and shared input from sources other than the stimulus.

The method described can be extended as follows: When more than two neurons are monitored together with a stimulus train, each spike train can be assigned its own Cartesian coordinate. The resulting $N$-dimensional scatter diagram, although presenting some difficulties in display, can be interpreted in a completely analogous manner to that of the two-dimensional diagrams. For example, a concentration of points about a line parallel to the principal diagonal of the coordinate system corresponds to a set of interactions, or shared input unrelated to the stimulus, involving all of the monitored neurons.

The scatter diagram described here is a supplement to rather than a substitute for the PST and cross-correlation histograms. Weak interactions may be more readily detected in the appropriate histogram. Examination of the histograms can serve as a guide to the detailed interpretation of particular features in the scatter diagram. This combined approach should be particularly applicable, for example, to experiments which seek to associate plasticity of behavior with changes in neuronal interactions.

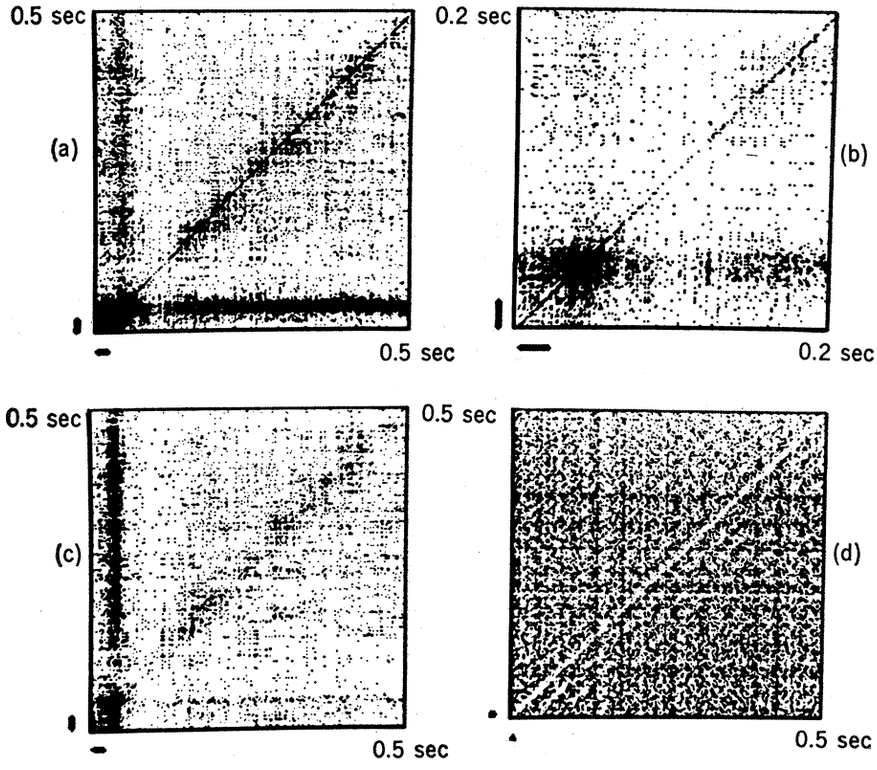


Fig. 2. Joint PST scatter diagrams. Units in auditory cortex of unanesthetized cat. Stimuli were 20-msec noise bursts, two per second, and are indicated by the dark bars. (a) Units 1 and 3: strong vertical and horizontal bands represent the stimulus-caused activity of each unit individually. The different latencies, time courses, and fine structures of the two responses are apparent. The narrow diagonal band represents a direct excitatory interaction between the two neurons with a latency of 3 msec. The wide diagonal band of increased density in central and upper right portion is most plausibly attributed to a weak shared excitatory input. The absence of this wide diagonal band in the lower left portion of scatter diagram indicates inhibition of the inferred common source for some time after the stimulus. (b) Enlargement of lower left portion of (a); differences in vertical and horizontal structure of region of high density and variation of density along the thin diagonal band, presumably reflecting stimulus-related reduction of firing, are shown. (c) Units 2 and 3, same preparation. The wide diagonal band again indicates that the stimulus inhibited shared input from nonstimulus sources. The shared input reaches unit 3 after unit 2, in that the wide diagonal band lies above the principal diagonal. There is no evidence for a direct synaptic connection. (d) Two Purkinje cells in the vermis of anesthetized cat cerebellum during an auditory stimulation by clicks (one click per second). There are no significant vertical or horizontal features, indicating that these units did not respond to the stimulus. Multiple diagonal bands are visible and presumably represent shared input and time delays associated with parallel-fiber input (*2*).


GEORGE L. GERSTEIN
*Departments of Biophysics* and *Physiology, University of Pennsylvania, Philadelphia 19104*

DONALD H. PERKEL
*Department of Mathematics, RAND Corporation, Santa Monica, California 90406*


### References and Notes


1. G. P. Moore, D. H. Perkel, J. P. Segundo, *Ann. Rev. Physiol.* **28**, 493 (1966).
2. D. H. Perkel, G. L. Gerstein, G. P. Moore, *Biophys. J.* **7**, 419 (1967).
3. We propose "peri-stimulus-time" instead of the older restrictive term "post-stimulus-time." The initials PST are thereby preserved.
4. The joint PST density may be defined by the equation

$$\xi_{ab}(t, u) = \lim_{\substack{\Delta t \to 0 \\ \Delta u \to 0}} \frac{1}{\Delta t\, \Delta u} P$$

where $P$ equals probability [spike in A in $(v + t, v + t + \Delta t)$ and spike in B in $(v + u, v + u + \Delta u)$, given the stimulus event at $v$]
5. C. C. Bell and R. J. Grimm, personal communication.


6. Supported by PHS grants NB 05606, NB 07325, FR-15, and by United States Air Force Project RAND.

6 February 1969


## Scanning Electron Microscopy of Cells


Abstract. *The scanning electron energy-analyzing microscope uses characteristic energy losses to provide picture contrast. At different levels of energy loss particular structures are distinguished with high contrast in an unstained section of a cell.*


Electron microscopy of ultrathin sections of biological tissue generally requires electron-opaque staining to obtain suitable contrast for detailed analysis. A heavy atom that selectively attaches to certain cell components (such as nuclei, mitochondria, and lysosomes) is typically used to stain the specimen. The contrast provided by such staining for examination with a conventional electron microscope depends primarily on specimen density. An ideal mechanism for obtaining contrast would be one in which different structures could be shown suc-